

Folate Receptor–Specific Antitumor Activity of EC131, a Folate-Maytansinoid Conjugate

Joseph A. Reddy,¹ Elaine Westrick,¹ Hari K.R. Santhapuram,¹ Stephen J. Howard,¹ Michael L. Miller,² Marilynn Vetzal,¹ Iontcho Vlahov,¹ Ravi V.J. Chari,² Victor S. Goldmacher,² and Christopher P. Leamon¹

¹Endocyte, Inc., West Lafayette, Indiana and ²ImmunoGen, Inc., Cambridge, Massachusetts

Abstract

EC131, a new folate receptor (FR)–targeted drug conjugate, was prepared by covalently attaching the vitamin folic acid (FA) to a potent microtubule-inhibiting agent, maytansinoid DM1, via an intramolecular disulfide bond. When tested on cells in culture, EC131 was found to retain high affinity for FR-positive cells and to provide FR-specific cytotoxicity with an IC_{50} in the low nanomolar range. The activity of EC131 was completely blocked in the presence of an excess of free FA, and no activity was detected against FR-negative cells. When evaluated against s.c. FR-positive M109 tumors in BALB/c mice, EC131 showed marked antitumor efficacy. Furthermore, this therapeutic effect occurred in the apparent absence of weight loss or noticeable organ tissue degeneration. In contrast, no significant antitumor activity was observed in EC131-treated animals that were codosed with an excess of FA, thus demonstrating the targeted specificity of the *in vivo* activity. EC131 also showed marked antitumor activity against FR-positive human KB tumors, but not against FR-negative A549 tumors, in nude mice with no evidence of systemic toxicity during or after the therapy. In contrast, therapy with the free maytansinoid drug (in the form of DM1-S-Me) proved not to be effective against the KB model when administered at its maximum tolerated dose (MTD). Taken together, these results indicate that EC131 is a highly potent agent capable of producing therapeutic benefit in murine tumor models at sub-MTD levels. [Cancer Res 2007;67(13):6376–82]

Introduction

Although considerable progress has been made in the development of anticancer therapies, cancer still remains a major cause of death in the United States. One of the challenging aspects of treating cancer has been the limitation on dosing of conventional chemotherapeutic agents because of their toxic side effects and, in particular, their toxicity toward actively proliferating nonmalignant cells.

The development of techniques to selectively target drug molecules to the tumor sites has allowed for enhancing the selectivity of anticancer drugs and simultaneously reducing unwanted systemic toxicity. This approach of targeting potent antiproliferative agents to the tumor by conjugating cytotoxic

drugs, such as doxorubicin (1, 2), maytansinoid DM1 (3–5), and CC-1065 analogue DC1 (6), to antibodies with affinity to a tumor-associated antigen has shown impressive preclinical antitumor activities; further, it has been validated by the recent approval of Mylotarg, an anti-CD33 monoclonal antibody (mAb)–calicheamicin conjugate, for the treatment of acute myeloid leukemia (7, 8). In principle, due to their larger molecular size, mAb–drug conjugates may have lower tumor penetration ability than that of a low-molecular-weight drug (9). Thus, we wished to test whether a low-molecular weight, high-affinity receptor targeting ligand linked to a potent cytotoxic drug would translate into high antitumor activity in animal models.

One example of a small-molecule targeting ligand system is that which uses folic acid (FA; or folate) to deliver chemically linked therapeutic or imaging agents to cells that express the FA receptor (FR; refs. 10–13). FA has high affinity ($K_d \sim 0.1$ – 1 nmol/L) for the FR, which is a protein expressed in high quantities by many primary and metastatic cancers (14–16) such as those originating in ovary, lung, breast, endometrium, kidney, and brain but not on most normal cells (17). FA has been used for the delivery of a wide range of drugs, and promising preclinical activity has recently been shown (10, 11, 13, 18–29). Because FA-linked molecules are efficiently bound to FRs and internalized by receptor-mediated endocytosis, we have explored the ability of FA to target the highly potent antitubulin agent, DM1, which is a derivative of the natural product, maytansine.

Maytansine, first isolated from *Maytenus ovatus* (30), is a well-investigated agent possessing very potent inhibitory action against the growth of cancer cells (31). Maytansine has been shown to inhibit the binding of the *Vinca* alkaloids to tubulin (32), and it acts as a mitotic inhibitor by interfering with the formation of microtubules (33). Although maytansine itself has not shown significant benefit in clinical trials as a cancer treatment (34), this compound still attracts considerable attention from many investigators, especially for its use as a conjugate with tumor-specific antibodies. Here, we report on our synthesis and preclinical investigation of EC131, a maytansinoid drug (DM1) linked to the small tumor-targeting ligand, FA.

Experimental Procedures

Materials. Pteric acid (Pte) and N^{10} -trifluoroacetylptericoic acid were prepared according to Xu et al. (35). Peptide synthesis reagents were purchased from NovaBiochem and Bachem. DM1 and DM1-S-Me were prepared from the microbial fermentation product Ansamitocin P-3 following literature procedures (36, 37). All other chemicals were of reagent grade and were obtained from major suppliers.

Synthesis, purification, and analytic characterization of EC131. EC131 was synthesized by constructing the FA and maytansinoid sections separately followed by a one-step conjugation. Synthesis of the FA-containing

Requests for reprints: Christopher P. Leamon, Endocyte, Inc., 3000 Kent Avenue, Suite A1-100, West Lafayette, IN 47906. Phone: 765-463-7175; Fax: 765-463-9271; E-mail: Chrisleamon@endocyte.com.

©2007 American Association for Cancer Research.
doi:10.1158/0008-5472.CAN-06-3894

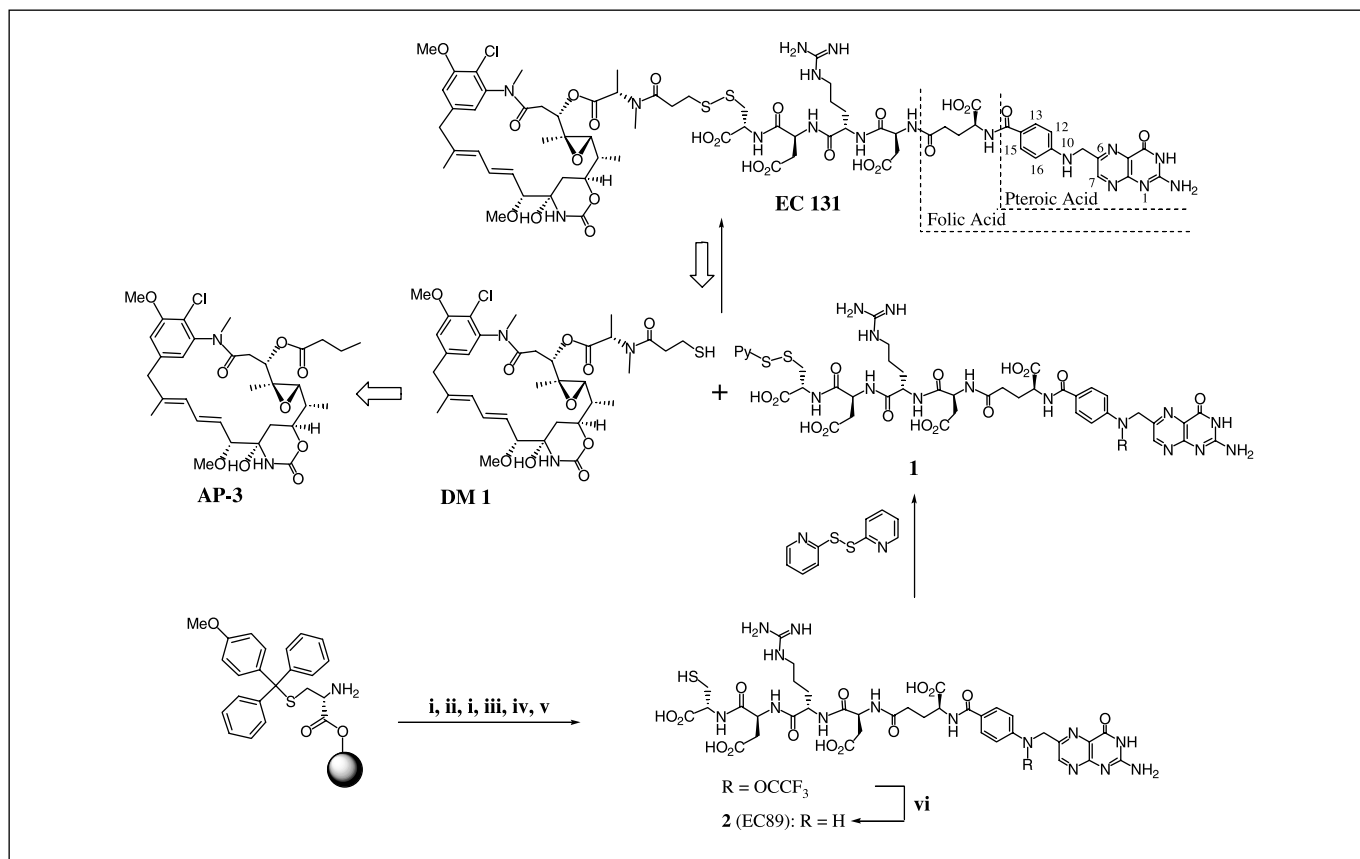


Figure 1. A retrosynthetic route for the synthesis of EC131. Reagents: *i*, Fmoc-Asp(OtBu)-OH, PyBOP, DIPEA; 20% piperidine/DMF. *ii*, Fmoc-Arg(Pbf)-OH, PyBOP, DIPEA; 20% piperidine/DMF. *iii*, Fmoc-Glu-OtBu, PyBOP, DIPEA; 20% piperidine/DMF. *iv*, *N*¹⁰-TFA-ptericoic acid, PyBOP, DIPEA. *v*, TFA/H₂O/TIPS/EDT (92.5:2.5:2.5:2.5). *vi*, aqueous NH₄OH (pH 9.3).

peptide spacer, EC89³ (Pte-γGlu-Asp-Arg-Asp-Cys; see Fig. 1, **2**), was done by using a preloaded Fmoc-Cys (Mmt) 2-chlorotrityl resin and standard solid-phase techniques. EC89 was purified on a preparative reversed-phase high-performance liquid chromatography (RP-HPLC) system connected to a Novapak HR C18 19 × 300 mm column. A gradient method was used, starting with 99% mobile phase A [10 mmol/L ammonium acetate buffer (pH 5.5)] and 1% mobile phase B (acetonitrile) and reaching 50% B within 30 min at a flow rate of 15 mL/min. Fractions corresponding to the main peak (UV monitoring at 280 nm) were combined, and the acetonitrile was removed under reduced pressure. The remaining solution was subjected to freeze drying for 48 h to give EC89 at >90% purity based on analytic RP-HPLC (room temperature 10 min) on NovaPak C18 3.9 × 150 mm column and using a gradient of solvents starting with 99% mobile phase A [10 mmol/L ammonium acetate buffer (pH 5.5)], 1% mobile phase B (acetonitrile), and reaching 50% B within 30 min at a flow rate of 1.0 mL/min. Electrospray-mass spectrometry (ESI-MS) analysis of EC89 identified the correct molecular ion (M + H)⁺ = 931. Next, 100 mg of EC89 were dissolved in 4 mL of water and triturated with argon for 10 min. In a separate flask, a 0.1 N NaHCO₃ solution was triturated with argon for 10 min. The pH of the EC89 solution was carefully adjusted to 6.9 using this 0.1 N NaHCO₃ solution. The dipyridyldisulfide reagent (30 mg, 1.25 equivalent) dissolved in 2 mL of acetonitrile was added slowly to the above solution. The resulting clear solution was stirred under argon for 15 min to 1 h. Progress of the reaction was monitored by analytic RP-HPLC [0.1% trifluoroacetic acid

(TFA) in water (pH 2.0) and acetonitrile]. The acetonitrile was removed under reduced pressure and the aqueous solution was filtered and injected on a preparative RP-HPLC column (Waters X-terra C₁₈ 300 × 19 mm). Elution with 0.1% TFA in water (pH 2.0) and acetonitrile resulted in pure fractions containing the product. Pure fractions were pooled, acetonitrile was removed under reduced pressure at ambient temperature, and the sample was freeze-dried for 48 h (70 mg, 63% yield, HPLC purity >90%). ESI-MS analysis of **1** correctly identified the molecular ion (M + H)⁺ = 1041.

Ansamitocin P-3 was converted to the thiol-containing maytansinoid DM1, and the methylthio-maytansinoid DM1-S-Me, as described previously (36, 37). DM1-S-Me, which is a stable form of DM1, was used as the free drug in efficacy studies in mice. DM1 was reacted with **1** to yield EC131 as follows: A solution of the pyridyldithio-activated EC89 **1** (6.5 mg, 6.26 mmol) in a 1:1 mixture of DMF (0.175 mL) and potassium phosphate buffer [50 mmol/L (pH 7.5), 0.175 mL] was stirred at room temperature. To this solution was added aqueous sodium bicarbonate (177 mmol/L, 30.5 mmol) with stirring. After stirring for 5 min, DM1 (5 mg, 6.1 mmol) dissolved in DMF (0.195 mL) was added. RP-HPLC analysis of the crude reaction confirmed that the reaction was complete after 30 min. The reaction was quenched with acetic acid (0.075 mL) to give a total volume of 0.750 mL. The solution was purified on RP-HPLC using a Vydac C18 column, eluting with a gradient of acetonitrile and water containing 0.02% formic acid. Fractions containing product were combined and concentrated under vacuum to give 4.24 mg of the desired product. Calculated *m/z* for C₇₁H₉₂ClN₁₇O₂₄S₂ is 1,665.56 (found 1,666.6).

Cell culture. Cells were grown continuously as a monolayer using FA-free RPMI medium (FFRPMI) containing 10% heat-inactivated FCS (HIFCS) at 37°C in a 5% CO₂/95% air-humidified atmosphere with no antibiotics. HIFCS contains endogenous FAs at concentrations sufficient for

³ EC89 consists of Pte-γGlu-Asp-Arg-Asp-Cys, which is the FA-peptide moiety found within EC131. Ptericoic acid, together with the NH₂-terminal γGlu residue of the peptide spacer module, constitutes the FA ligand.

FR-expressing cells to survive and proliferate in this medium (18), which consequently is more physiologically relevant than typical cell culture medium that contains 100- to 1,000-fold higher levels of FAs. All cell culture experiments were done using FFRPMI containing 10% HIFCS (FFRPMI/HIFCS) as the growth medium.

Relative affinity assay. The relative affinity of EC131 was determined according to the method described by Westerhoff et al. (38) with slight modification. Briefly, FR-positive KB cells were seeded in 24-well Falcon plates and allowed to form adherent monolayers (>90% confluent) overnight in FFRPMI/HIFCS. Spent incubation medium was replaced with FFRPMI supplemented with 10% HIFCS and containing 100 nmol/L of [³H]FA in the absence and presence of increasing concentrations of unlabeled FA or EC131. Cells were incubated for 1 h at 37°C and then rinsed thrice with 0.5 mL PBS. Five hundred microliters of 1% SDS in PBS were added to each well; after 5 min, cell lysates were collected, transferred to individual vials containing 5 mL of scintillation cocktail, and then counted for radioactivity. Cells exposed to only the [³H]FA in FFRPMI (no competitor) were designated as negative controls, whereas cells exposed to the [³H]FA plus 1 mmol/L unlabeled FA served as positive controls. Disintegrations per minute (DPM) measured in the latter samples (representing nonspecific binding of label; 826 DPM) were subtracted from the DPM values from all samples. Notably, relative affinities were defined as the inverse molar ratio of compound required to displace 50% of [³H]FA bound to FR on KB cells, and the relative affinity of FA for the FR was set to 1.

Dose-dependent FR-specific activity of EC131. FR-positive KB (human nasopharyngeal carcinoma), ID8 Clone-15 (stable FR transfected murine ovarian cancer), New Line-01 (mouse lung cancer) and M109 (murine lung adenocarcinoma) or FR-negative 4T1 (mouse breast cancer), CHO (Chinese hamster ovarian cancer), 24JK (mouse sarcoma), and A549 (human lung carcinoma) cells were seeded in 12-well Falcon plates and allowed to form nearly confluent monolayers overnight in FFRPMI/HIFCS. Thirty minutes before the addition of EC131, spent medium was aspirated from all wells and replaced with either fresh FFRPMI or FFRPMI supplemented with 100 μmol/L FA. At this concentration, free FA completely blocked the binding of EC131 to FR on the cell surface, thus revealing the extent of nontargeted FR-independent cytotoxicity of EC131. Each well then received 1 mL of medium containing increasing concentrations of EC131 (four wells per sample). Cells were pulsed for 1 h at 37°C, rinsed four times with 0.5 mL of medium, and then chased in 1 mL of fresh medium up to 72 h. Spent medium was aspirated from all wells and replaced with fresh medium containing 5 μCi/mL of [³H]thymidine. Following a 2 h incubation at 37°C, cells were washed thrice with 0.5 mL of PBS and then treated with 0.5 mL of

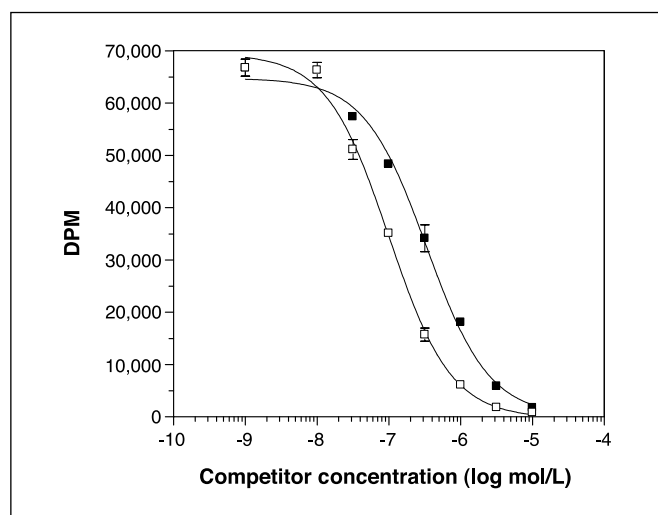


Figure 2. Relative folate receptor binding affinity of EC131. KB cells were incubated for 1 h at 37°C with 100 nmol/L [³H]FA in the presence and absence of increasing competitor concentrations. □, FA; ■, EC131. Bars, 1 SD ($n = 3$).

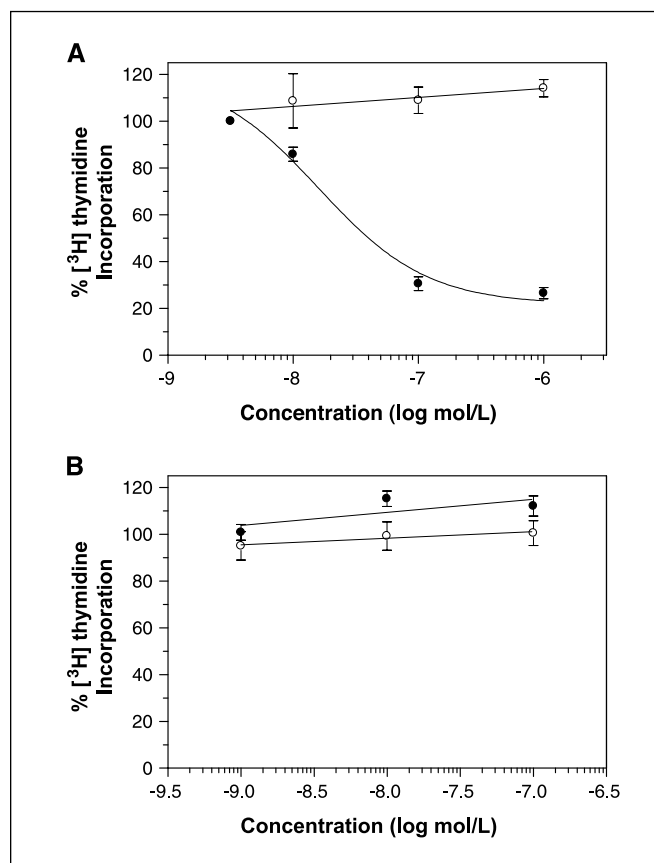


Figure 3. EC131 dose response. FR-positive KB cells (A) or FR-negative 4T1 cells (B) were treated for 1 h with increasing concentrations of EC131 in the presence (○) or absence (●) of 100 μmol/L FA (as a competitor). Following a 70 h chase in fresh medium, cells were incubated with [³H]thymidine for 2 h and then counted for radiolabel incorporation into newly synthesized DNA, as described in Experimental Procedures. Points, average ($n = 4$); bars, SD.

ice-cold 5% trichloroacetic acid per well. After 15 min, the trichloroacetic acid was aspirated and the cells were solubilized by the addition of 0.5 mL of 0.25 N sodium hydroxide for 15 min at room temperature. Four hundred and fifty microliters of each solubilized sample were transferred to scintillation vials containing 3 mL of Ecolume scintillation cocktail and counted in a liquid scintillation counter. Final results were expressed as the percentage of [³H]thymidine incorporation (39) relative to untreated controls.

Tumor models and therapy. Six- to eight-week-old female BALB/c mice (Harlan Sprague-Dawley, Inc.) or female *nu/nu* mice (Charles River) were maintained on a standard 12 h light-dark cycle for the duration of the experiment. Because normal rodent chow contains a high concentration of FA (6 mg/kg chow), mice used in these studies were fed a FA-free diet (Harlan diet TD00434, Harlan Teklad) beginning 2 weeks before tumor implantation and maintained throughout the experiment to achieve serum FA concentrations closer to the range of normal human serum (40). Syngeneic, FR-positive M109 tumor cells (1×10^6 per BALB/c mouse) or FR-positive KB cells (1×10^6 per *nu/nu* mouse) or FR-negative A549 tumor cells (1×10^6 per *nu/nu* mouse) in 100 μL of FFRPMI containing 1% BALB/c serum were injected in the subcutis of the dorsal medial area. Tumors were measured in two perpendicular directions every 2 to 3 days using a caliper and their volumes were calculated as $0.5 \times L \times W^2$, where L is the measurement of longest axis in millimeters and W is the measurement of axis perpendicular to L in millimeters. Data were analyzed using one-way ANOVA by comparing the dose groups at each time point. Differences between groups were considered statistically significant at $P \leq 0.05$. Log cell

kill (LCK) and treated over control (T/C) values were then calculated according to published procedures (41, 42).

Dosing solutions were prepared fresh each day in PBS and administered through the lateral tail vein of the mice. Importantly, dosing was initiated when the s.c. tumors were between 50 and 100 mm³ in volume. Drug toxicity was assessed by collecting blood via cardiac puncture and submitting the sera for independent analysis of blood urea nitrogen, creatinine, and the liver enzymes aspartate aminotransferase (AST-SGOT) and alanine aminotransferase (ALT-SGPT) at Ani-Lytics, Inc. In addition, histopathologic evaluation of formalin-fixed heart, lungs, liver, spleen, kidney, intestine, skeletal muscle, and bone (tibia/fibula) were done at Animal Reference Pathology Laboratories (ARUP, Salt Lake City, UT).

Results

Synthesis of EC131. The design and regioselective synthesis of the DM1 conjugate, EC131, is outlined in Fig. 1. As indicated in the retrosynthetic analysis, EC131 was assembled by tethering the FA-peptide unit, EC89, **2**, to the maytansinoid DM1, via a reducible disulfide bond.

Relative affinity assay. The binding affinity of EC131, relative to FA, was evaluated using an *in vitro* competition assay. As shown in Fig. 2, the affinity of EC131 toward the FR was determined to be ~2.7-fold lower than that of FA (0.37 relative to FA). Thus, linkage of a large maytansinoid molecule does not radically alter the vitamin's intrinsic binding affinity to its receptor.

***In vitro* cytotoxicity and specificity.** The cytotoxicity of EC131 was evaluated against a panel of FR-positive (>6 pmol FR/mg protein, as defined in ref. 17) and FR-negative (<2.5 pmol FR/mg protein) cells *in vitro*. As shown in Fig. 3A, EC131 was determined to be highly cytotoxic toward KB cells, with an IC₅₀ value of 16 nmol/L. This activity was completely blocked by excess FA, thereby demonstrating that the cytotoxic effect was FR mediated. The activity of EC131 was also determined to be concentration dependent against FR-positive ID8 Clone-15, New Line-01, and M109 cells with IC₅₀ values <25 nmol/L (Table 1). This activity was again effectively blocked in the presence of excess free FA. In addition, EC131 was not found to be cytotoxic toward FR-negative 4T1 (Fig. 3B), CHO, 24JK, or A549 cells (see Table 1) within the range of concentrations tested, which further substantiates the selective action of the drug toward FR-positive cells.

FR-specific *in vivo* potency of EC131. The antitumor activity of EC131 was examined against BALB/c mice bearing the s.c. FR-

positive syngeneic lung adenocarcinoma, M109, which incidentally express similar numbers of receptors as many human ovarian carcinomas (17). The activity of EC131 was first assessed by administering the drug i.v. 11 days post tumor implantation (PTI) using a 1 μmol/kg dose level and following a twice weekly, 4-week-long treatment schedule. As shown in Fig. 4A, tumors in the untreated animals reached ~1,500 mm³ by approximately day 42, whereas the tumor growth in animals treated with EC131 was markedly delayed (on the average, by ~45 days). Out of five animals treated with EC131, one mouse experienced a complete response (CR), three mice had partial responses (PR) with a collective LCK of 1.2 and 181% T/C, and one of the five mice did not respond. The EC131 group differed significantly from that of the untreated group at days 18 PTI and beyond. Importantly, at this dose of EC131, the animals experienced no noticeable toxicity (see below). The antitumor activity of EC131 was essentially eliminated when this agent was coadministered together with a 10-fold molar excess of unmodified FA (i.e., no CR or PR among five animals; an average tumor growth delay of only 1 day; see Fig. 4A) with statistically significant differences being achieved between the two groups at day 25 PTI and beyond. This outcome indicated that the antitumor activity of EC131 was dependent on its binding to tumor-associated FR. Free drug (as DM1-S-Me) was administered to mice at its maximum tolerated dose (MTD) of 1 μmol/kg twice a week. This treatment resulted in only a modest 8-day average delay of tumor growth (Fig. 4A) producing one CR, whereas the other four animals did not respond to the treatment. Overall, the antitumor effects in the EC131 group differed significantly from that of the DM1-S-Me-treated group at days 32 PTI and beyond.

A second study was done in *nu/nu* mice bearing a s.c. xenograft of FR-positive human KB tumor. Animals were treated i.v. with 1.5 μmol/kg of EC131 given thrice a week for a total of 3 weeks starting 11 days PTI. In this model, EC131 was also found to produce marked antitumor activity, delaying the tumor growth by at least 55 days (Fig. 5A) with four CRs and one PR (0.9 LCK and 156% T/C). Again, not one of the EC131-treated animals showed any signs of toxicity during and after the therapy. In contrast to EC131, DM1-S-Me dosed at its MTD (0.12 μmol/kg, daily × 5, 1 week schedule) did not produce any meaningful antitumor activity in this xenograft model (0 CR and PR; collective LCK of 0.3 and 119% T/C; see Fig. 5B). Thus, for a second time, the antitumor effect in the EC131

Table 1. Specific activity of EC131 against a panel of cell lines

FR status	Tumor cell type	Species	FR level (pmol/mg membrane protein)	IC ₅₀ (nmol/L)*	
				EC131	EC131 + excess FA
FR positive	KB	Human	80.0	16	>1,000
	New Line-01	Murine	49.4	16	>1,000
	ID8 Clone-15	Murine	44.7	14	>1,000
	M109	Murine	44.5	25	>1,000
FR negative	A549	Human	1.3	>1,000	>1,000
	24JK	Murine	1.0	>1,000	>1,000
	4T1	Murine	0.3	>1,000	>1,000
	CHO	Hamster	0.0	>1,000	>1,000

*One hour pulse with EC131, 70 h chase in fresh medium.

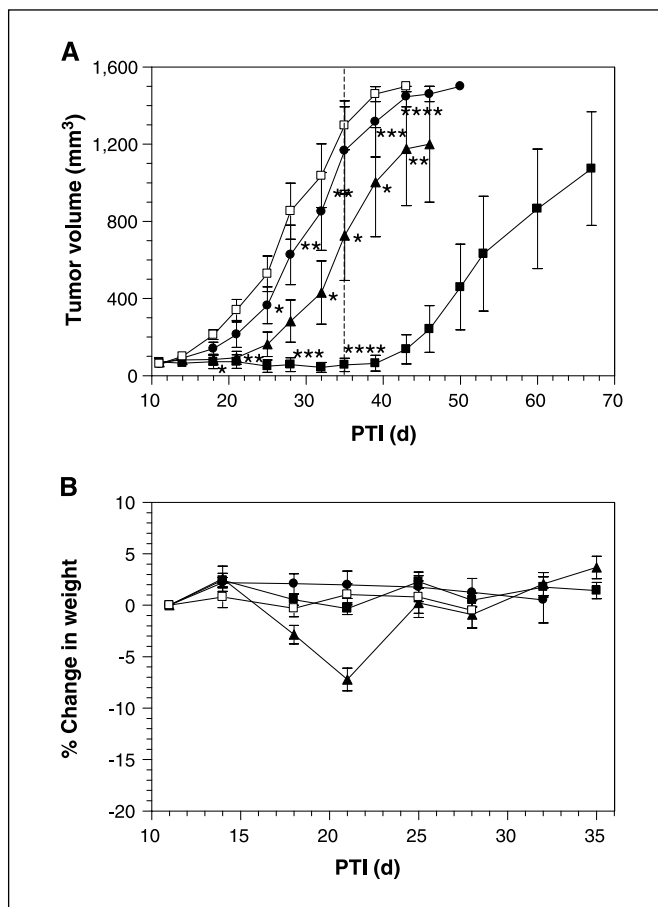


Figure 4. Effect of EC131 on the growth of s.c. FR-positive M109 tumors (A) and on weight of the treated BALB/c mice (B). M109 tumor cells (1×10^6) were implanted s.c. into BALB/c mice, and 11 d later, mice were randomized and treatments given i.v. ($1 \mu\text{mol/kg/injection}$) on a twice a week schedule for 4 wks. \square , untreated mice; \blacksquare , EC131-treated mice (statistical comparison with untreated mice); \bullet , EC131-treated group coinjected with $10 \mu\text{mol/kg/injection}$ of FA (statistical comparison with EC131-treated mice); \blacktriangle , DM1-S-Me maytansinoid administered at $1 \mu\text{mol/kg/injection}$ on a twice a week schedule for a total of three doses (statistical comparison with EC131-treated mice). Points, average tumor volume from five animals. Dotted vertical line, day of final dosing for the EC131 and EC131 + FA cohorts (day 35). Data were analyzed using one-way ANOVA (*, $P < 0.05$; **, $P < 0.01$; ***, $P < 0.001$; ****, $P < 0.0001$).

group differed significantly from that of the untreated group and the DM1-S-Me-treated groups at days 18 PTI and beyond.

An additional control study was done where *nu/nu* mice were inoculated with s.c. FR-negative A549 human cancer cells and then subsequently treated with i.v. EC131 injections 15 days after tumor cell inoculation using either a $1 \mu\text{mol/kg}$, BIW \times 4 week regimen (similar to M109 tumor study; Fig. 4), or a $1.5 \mu\text{mol/kg}$, TIW \times 3 week regimen (similar to KB tumor study; Fig. 5). In either case, EC131 did not produce any significant antitumor effect (Fig. 6A). Thus, together with the M109 and KB model data, these data confirm that the *in vivo* activity of EC131 is potent and specific for FR-expressing tumors.

Treatment-related adverse events. To evaluate the systemic toxicity of the EC131 and DM1-S-Me therapies, the tumor-bearing BALB/c and *nu/nu* mice were monitored during and after the time of treatment for changes in motor and feeding behavior, body weight, serum markers, and histopathology of important tissues.

Motor activity and feeding behavior of all EC131-treated mice were completely normal throughout the duration of the study. As shown in Figs. 4B and 5B, the body weights of the mice treated with EC131 remained stable throughout the experiments. In contrast, BALB/c mice treated with untargeted DM1-S-Me had lost 5% to 10% weight after receiving only three doses.

Serum samples were analyzed for changes in clinical chemistry markers. The amounts of ALT, creatinine, blood urea nitrogen, and total protein were found to be within normal levels in all of the EC131-treated BALB/c and *nu/nu* mice. The liver enzyme AST was modestly elevated (≈ 1.7 -fold of the upper reference limit) in EC131-treated BALB/c mice. The corresponding DM1-S-Me-treated mice displayed up to 2-fold elevation of aspartate aminotransferase.

Histopathologic evaluation of the liver, spleen, intestine, bone, and kidneys of both BALB/c and *nu/nu* mice treated with EC131 were all normal. Mild degeneration was observed in the livers of the DM1-S-Me-treated mice. Taken together, the morbidity, mortality, serum markers, and pathologic observations showed that the EC131 therapy was well tolerated at therapeutically effective dose levels.

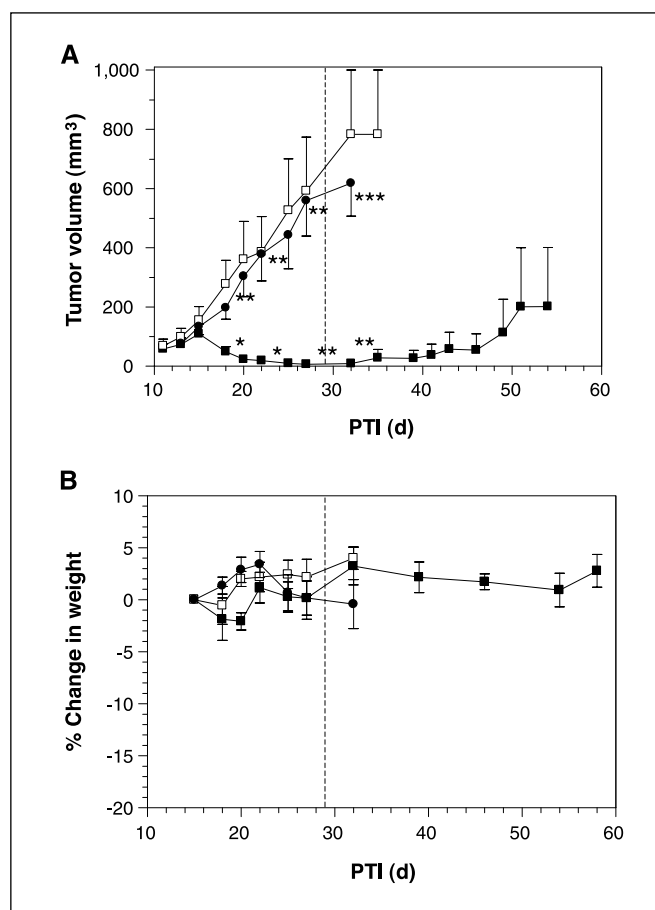


Figure 5. Effect of EC131 on the growth of s.c. FR-positive KB tumors (A) and on weight of the treated *nu/nu* mice (B). KB tumor cells (1×10^6) were implanted s.c. into *nu/nu* mice, and 11 d later, mice were randomized and treatments given ($1.5 \mu\text{mol/kg/injection}$) following a thrice per week, 3 wks schedule. \square , untreated mice; \blacksquare , EC131-treated group (statistical comparison with untreated mice); \bullet , DM1-S-Me maytansinoid administered at $0.12 \mu\text{mol/kg/injection}$, on a qd \times 5, 1 wk schedule (statistical comparison with EC131-treated mice). Points, an average tumor volume from five animals. Dotted vertical line, day of final dosing for the EC131 cohort (day 29). Data were analyzed using one-way ANOVA (*, $P < 0.05$; **, $P < 0.01$; ***, $P < 0.001$).

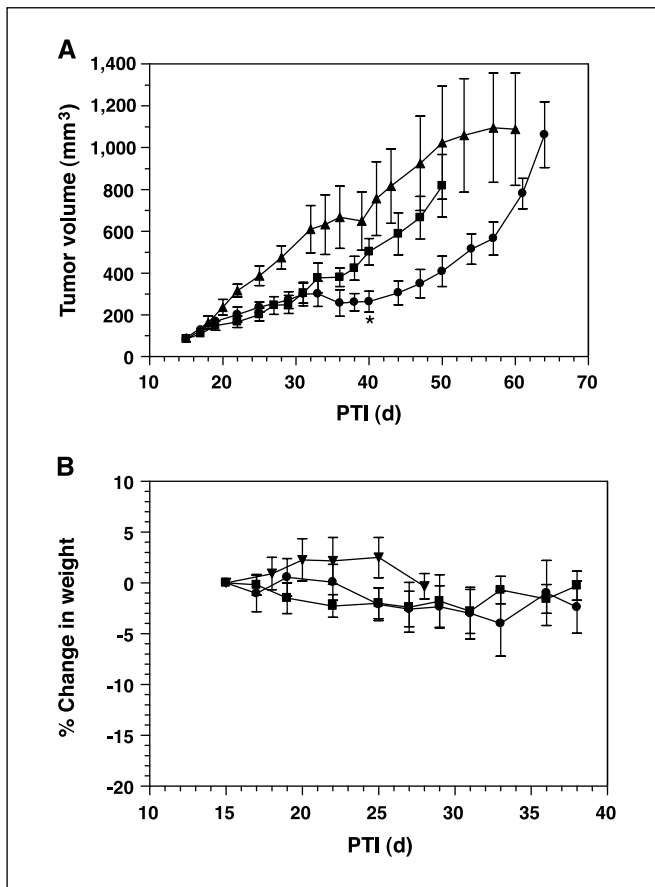


Figure 6. Effect of EC131 on the growth of s.c. FR-negative A549 tumors (A) and on weight of the treated *nu/nu* mice (B). A549 tumor cells (1×10^6) were implanted s.c. into *nu/nu* mice, and 15 d later, mice were randomized and treated with EC131. ■, untreated mice; ▲, EC131-treated group at 1 $\mu\text{mol/kg}$ /injection on a twice a week schedule for 4 wks; ●, EC131-treated group at 1.5 $\mu\text{mol/kg}$ /injection following a thrice per week, 3 wks schedule (statistical comparison with controls). Points, average tumor volume from five animals. Data were analyzed using one-way ANOVA (*, $P < 0.05$).

Discussion

EC131 is a novel conjugate of FA with the potent maytansinoid DM1 drug linked together with a disulfide bond. It has been recently shown (43, 44) that linkers of this type are stable in the circulation for a prolonged period of time, but are cleaved inside the cell, releasing a free cytotoxic derivative of maytansinoid. Notably, intracellular release of disulfide-linked drugs from a FA conjugate was recently shown by real-time imaging using a fluorescence resonance energy transfer technique (45).

A previously reported FA-maytansinoid conjugate (25), although found to be potent *in vitro*, was never tested *in vivo* due to poor water solubility. To circumvent this issue, we used an improved, highly water soluble peptide spacer for construction of EC131.

References

- Trail PA, Willner D, Lasch SJ, et al. Cure of xenografted human carcinomas by BR96-doxorubicin immunoconjugates. *Science* 1993;261:212–5.
- Tolcher AW, Sugarman S, Gelmon KA, et al. Random-

- ized phase II study of BR96-doxorubicin conjugate in patients with metastatic breast cancer. *J Clin Oncol* 1999;17:478–84.
- Liu C, Tadayoni BM, Bourret LA, et al. Eradication of large colon tumor xenografts by targeted delivery of maytansinoids. *Proc Natl Acad Sci U S A* 1996;93:8618–23.

4. Tolcher AW, Ochoa L, Hammond LA, et al. Cantuzumab mertansine, a maytansinoid immunoconjugate directed to the CanAg antigen: a phase I, pharmacokinetic, and biologic correlative study. *J Clin Oncol* 2003; 21:211–22.
5. Tassone P, Gozzini A, Goldmacher V, et al. *In vitro*

Importantly, FA-drug conjugates constructed with comparable hydrophilic spacers were recently found to be active against FR-expressing tumors (26–29, 46). Similarly, EC131 was found to produce a marked antitumor effect, selectively eradicating FR-expressing tumors in multiple mouse models.

The majority of normal tissues in the body express low to nondetectable levels of the FR (17). However, the proximal tubules of the kidney do express a substantial amount of this protein (14, 47, 48). The FR is restricted to the apical membrane of these polarized epithelial cells (i.e., facing the lumen of the tubule), and these sites are accessible to i.v. administered FA conjugates (14, 47, 49, 50). Overall, the function of kidney FRs seems to be to capture FAs, or drug conjugates thereof, in the urinary filtrate and to transcytose them back into the blood (47, 48, 51). Supporting this hypothesis are the observations that (a) analyses of blood from animals after i.v. therapy with FA-drug conjugates such as the FA-maytansinoid conjugate described above, FA-mitomycin C, and FA-*Vinca* alkaloids, have not detected any abnormalities in blood urea nitrogen or creatinine levels, and (b) pathologic analyses of kidneys from treated animals have not reported any apparent organ degeneration (26, 27). However, more thorough toxicologic studies are needed to affirm this premise.

A sizable number of antibody-drug conjugates are in preclinical and clinical evaluation. In such conjugates, the linked cytotoxic drug acquires the pharmacokinetic properties of the antibody component, such as a long serum half-life. With the use of small targeting molecules, such as FA, the cytotoxic drug maintains more of its drug-like pharmacokinetic characteristics, which may facilitate more extensive drug delivery to the tumor and, consequently, greater tumor cell kill. Because EC131 has been constructed with a highly hydrophilic peptide spacer, the increased water solubility could possibly allow for rapid penetration through interstitial spaces. Indeed, other hydrophilic FA-drug conjugates have shown the ability to rapidly saturate tumor-bound FRs, and to simultaneously clear from the blood stream (serum half lives are typically <5 min; refs. 49, 50). Such target-tissue-specific retention, with concomitant rapid clearance from circulation, may be viewed as favorable attributes to the FA-targeted therapeutic approach.

Considering that (a) a substantial number of tumor types have been reported to express the FR (14–16), and (b) the preclinical data from this study that show that DM1 can be effectively targeted to FR-positive tumors without significant toxicity, it is possible that EC131 could provide clinical benefit to FR-positive cancer patients.

Acknowledgments

Received 10/19/2006; revised 4/3/2007; accepted 5/2/2007.

The costs of publication of this article were defrayed in part by the payment of page charges. This article must therefore be hereby marked *advertisement* in accordance with 18 U.S.C. Section 1734 solely to indicate this fact.

We thank Dr. Philip S. Low for his valuable comments, and Nikki Parker for FR quantitation.

- and *in vivo* activity of the maytansinoid immunoconjugate huN901-2'-deacetyl-N²-(3-mercapto-1-oxo-propyl)-maytansine against CD56⁺ multiple myeloma cells. *Cancer Res* 2004;64:4629-36.
6. Chari RV, Jackel KA, Bourret LA, et al. Enhancement of the selectivity and antitumor efficacy of a CC-1065 analogue through immunoconjugate formation. *Cancer Res* 1995;55:4079-84.
 7. Damle NK, Frost P. Antibody-targeted chemotherapy with immunoconjugates of calicheamicin. *Curr Opin Pharmacol* 2003;3:386-90.
 8. Giles F, Estey E, O'Brien S. Gemtuzumab ozogamicin in the treatment of acute myeloid leukemia. *Cancer* 2003;98:2095-104.
 9. Jain RK. Delivery of molecular and cellular medicine to solid tumors. *Adv Drug Deliv Rev* 2001;46:149-68.
 10. Reddy JA, Allagadda VM, Leamon CP. Targeting therapeutic and imaging agents to folate receptor positive tumors. *Curr Pharm Biotechnol* 2005;6:131-50.
 11. Reddy JA, Low PS. Folate-mediated targeting of therapeutic and imaging agents to cancers. *Crit Rev Ther Drug Carrier Syst* 1998;15:587-627.
 12. Leamon CP, Low PS. Folate-mediated targeting: from diagnostics to drug and gene delivery. *Drug Discov Today* 2001;6:44-51.
 13. Reddy JA, Leamon CP, Low PS. Folate-mediated delivery of protein and peptide drugs into tumors. In: Torchilin V, editor. *Delivery of protein and peptide drugs in cancer*. London: World Scientific/Imperial College Press; 2006. p. 183-204.
 14. Weitman SD, Lark RH, Coney LR, et al. Distribution of the folate receptor GP38 in normal and malignant cell lines and tissues. *Cancer Res* 1992;52:3396-401.
 15. Ross JF, Chaudhuri PK, Ratnam M. Differential regulation of folate receptor isoforms in normal and malignant tissues *in vivo* and in established cell lines. *Physiologic and clinical implications*. *Cancer* 1994;73:2432-43.
 16. Toffoli G, Cernigoi C, Russo A, Gallo A, Bagnoli M, Boiocchi M. Overexpression of folate binding protein in ovarian cancers. *Int J Cancer* 1997;74:193-8.
 17. Parker N, Turk MJ, Westrick E, Lewis JD, Low PS, Leamon CP. Folate receptor expression in carcinomas and normal tissues determined by a quantitative radioligand binding assay. *Anal Biochem* 2005;338:284-93.
 18. Leamon CP, Low PS. Delivery of macromolecules into living cells: a method that exploits folate receptor endocytosis. *Proc Natl Acad Sci U S A* 1991;88:5572-6.
 19. Leamon CP, Low PS. Membrane folate-binding proteins are responsible for folate-protein conjugate endocytosis into cultured cells. *Biochem J* 1993;291:855-60.
 20. Rund LA, Cho BK, Manning TC, Holler PD, Roy EJ, Kranz DM. Bispecific agents target endogenous murine T cells against human tumor xenografts. *Int J Cancer* 1999;83:141-9.
 21. Lu Y, Low PS. Folate targeting of haptens to cancer cell surfaces mediates immunotherapy of syngeneic murine tumors. *Cancer Immunol Immunother* 2002;51:153-62.
 22. Lee RJ, Low PS. Delivery of liposomes into cultured KB cells via folate receptor-mediated endocytosis. *J Biol Chem* 1994;269:3198-204.
 23. Reddy JA, Abburi C, Hofland H, et al. Folate-targeted, cationic liposome-mediated gene transfer into disseminated peritoneal tumors. *Gene Ther* 2002;9:1542-50.
 24. Reddy JA, Xu LC, Parker N, Vetzal M, Leamon CP. Preclinical evaluation of (99m)Tc-EC20 for imaging folate receptor-positive tumors. *J Nucl Med* 2004;45:857-66.
 25. Ladino CA, Chari RV, Bourret LA, Kedersha NL, Goldmacher VS. Folate-maytansinoids: target-selective drugs of low molecular weight. *Int J Cancer* 1997;73:859-64.
 26. Reddy JA, Westrick E, Vlahov I, Howard SJ, Santhapuram HK, Leamon CP. Folate receptor specific anti-tumor activity of folate-mitomycin conjugates. *Cancer Chemother Pharmacol* 2006;58:229-36.
 27. Leamon CP, Reddy JA, Vlahov IR, Kleindl PJ, Vetzal M, Westrick E. Synthesis and biological evaluation of EC140: a novel folate-targeted *Vinca* alkaloid conjugate. *Bioconjug Chem* 2006;17:1226-32.
 28. Leamon CP, Reddy JA, Vlahov IR, et al. Comparative preclinical activity of the folate-*Vinca* alkaloid conjugates EC140 and EC145. *Int J Cancer*. In press 2007.
 29. Reddy JA, Dorton R, Westrick E, et al. Pre-clinical evaluation of EC145, a folate-*Vinca* alkaloid conjugate. *Cancer Res* 2007;67:4434-42.
 30. Kupchan SM, Komoda Y, Court WA, et al. Maytansine, a novel antileukemic ansa macrolide from *Maytenus ovatus*. *J Am Chem Soc* 1972;94:1354-6.
 31. Cassady JM, Chan KK, Floss HG, Leistner E. Recent developments in the maytansinoid antitumor agents. *Chem Pharm Bull (Tokyo)* 2004;52:1-26.
 32. Roach MC, Luduena RF. Different effects of tubulin ligands on the intrachain cross-linking of β 1-tubulin. *J Biol Chem* 1984;259:12063-71.
 33. Remillard S, Rebhun LI, Howie GA, Kupchan SM. Antimitotic activity of the potent tumor inhibitor maytansine. *Science* 1975;189:1002-5.
 34. Ravry MJ, Omura GA, Birch R. Phase II evaluation of maytansine (NSC 153858) in advanced cancer. A Southeastern Cancer Study Group trial. *Am J Clin Oncol* 1985;8:148-50.
 35. Xu L, Vlahov IR, Leamon CP, Santhapuram HKR, Li CH, inventors; Endocyte, Inc., assignee. Synthesis and purification of ptericoic acid and conjugates thereof. United States patent 2006.
 36. Chari RV, Martell BA, Gross JL, et al. Immunoconjugates containing novel maytansinoids: promising anticancer drugs. *Cancer Res* 1992;52:127-31.
 37. Widdison WC, Wilhelm SD, Cavanagh EE, et al. Semisynthetic maytansine analogues for the targeted treatment of cancer. *J Med Chem* 2006;49:4392-408.
 38. Westerhof GR, Schornagel JH, Kathmann I, et al. Carrier- and receptor-mediated transport of folate antagonists targeting folate-dependent enzymes: correlates of molecular-structure and biological activity. *Mol Pharmacol* 1995;48:459-71.
 39. Arnould R, Dubois J, Abikhail F, et al. Comparison of two cytotoxicity assays-tetrazolium derivative reduction (MTT) and tritiated thymidine uptake-on three malignant mouse cell lines using chemotherapeutic agents and investigational drugs. *Anticancer Res* 1990;10:145-54.
 40. Mathias CJ, Wang S, Lee RJ, Waters DJ, Low PS, Green MA. Tumor-selective radiopharmaceutical targeting via receptor-mediated endocytosis of gallium-67-deferoxamine-folate. *J Nucl Med* 1996;37:1003-8.
 41. Lee FY, Borzilleri R, Fairchild CR, et al. BMS-247550: a novel epothilone analog with a mode of action similar to paclitaxel but possessing superior antitumor efficacy. *Clin Cancer Res* 2001;7:1429-37.
 42. Rose WC. Taxol-based combination chemotherapy and other *in vivo* preclinical antitumor studies. *J Natl Cancer Inst Monogr* 1993;47-53.
 43. Xie H, Audette C, Hoffee M, Lambert JM, Blattler WA. Pharmacokinetics and biodistribution of the antitumor immunoconjugate, cantuzumab mertansine (huC242-1), and its two components in mice. *J Pharmacol Exp Ther* 2004;308:1073-82.
 44. Erickson HK, Park PU, Widdison WC, et al. Antibody-maytansinoid conjugates are activated in targeted cancer cells by lysosomal degradation and linker-dependent intracellular processing. *Cancer Res* 2006;66:4426-33.
 45. Yang J, Chen H, Vlahov IR, Cheng JX, Low PS. Evaluation of disulfide reduction during receptor-mediated endocytosis by using FRET imaging. *Proc Natl Acad Sci U S A* 2006;103:13872-7.
 46. Leamon CP, Reddy JA, Vlahov IR, et al. Synthesis and biological evaluation of EC72: a new folate-targeted chemotherapeutic. *Bioconjug Chem* 2005;16:803-11.
 47. Birn H, Selhub J, Christensen EI. Internalization and intracellular transport of folate-binding protein in rat kidney proximal tubule. *Am J Physiol* 1993;264:C302-10.
 48. Birn H, Nielsen S, Christensen EI. Internalization and apical-to-basolateral transport of folate in rat kidney proximal tubule. *Am J Physiol* 1997;272:F70-8.
 49. Leamon CP, Parker MA, Vlahov IR, et al. Synthesis and biological evaluation of EC20: a new folate-derived, (99m)Tc-based radiopharmaceutical. *Bioconjug Chem* 2002;13:1200-10.
 50. Mathias CJ, Wang S, Waters DJ, Turek JJ, Low PS, Green MA. Indium-111-DTPA-folate as a potential folate-receptor-targeted radiopharmaceutical. *J Nucl Med* 1998;39:1579-85.
 51. Morshed KM, Ross DM, McMartin KE. Folate transport proteins mediate the bidirectional transport of 5-methyltetrahydrofolate in cultured human proximal tubule cells. *J Nutr* 1997;127:1137-47.